Chemistry–A European Journal

Supporting Information

Anilato-Based Coordination Polymers with Slow Relaxation of the Magnetization: Role of the Synthetic Method and Anilato Ligand

Samia Benmansour,* Cristina Pintado-Zaldo, Sofía H. Casal-García, Javier Martínez-Ponce, and Carlos J. Gómez-García*

Electronic Supporting Information

Anilato-based Coordination Polymers with Slow Relaxation of the Magnetization: Role of the Synthetic Method and Anilato ligand

Samia Benmansour,*[a] Cristina Pintado-Zaldo,[a] Sofía H. Casal-García,[a] Javier Martínez-Ponce[a] and Carlos J. Gómez-García*[a]

[a] Departmento de Química Inorgánica. Facultad de Química. Universidad de Valencia. Dr. Moliner 50. 46100 Burjasot (Valencia) Spain E-mail: sam.ben@uv.es (SB) and carlos.gomez@uv.es (CJGG).

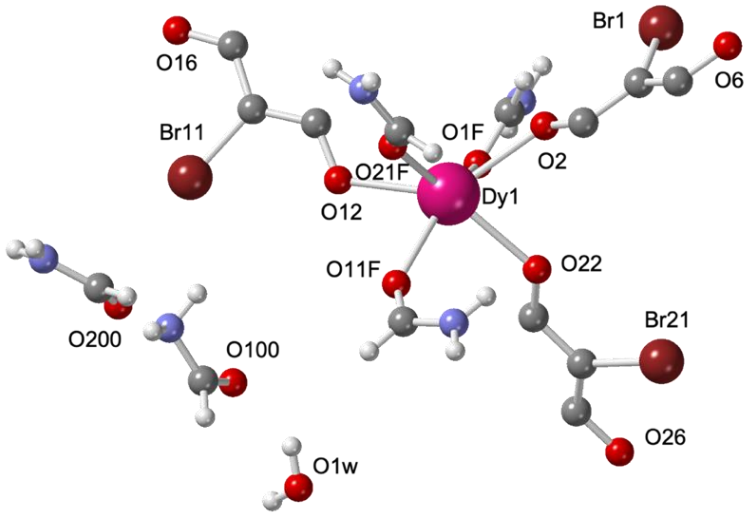

Figure S1. Asymmetric unit of compound $[Dy_2(C_6O_4Br_2)_3(fma)_6]\cdot 4fma\cdot 2H_2O$ (**2**) showing the labelling scheme.

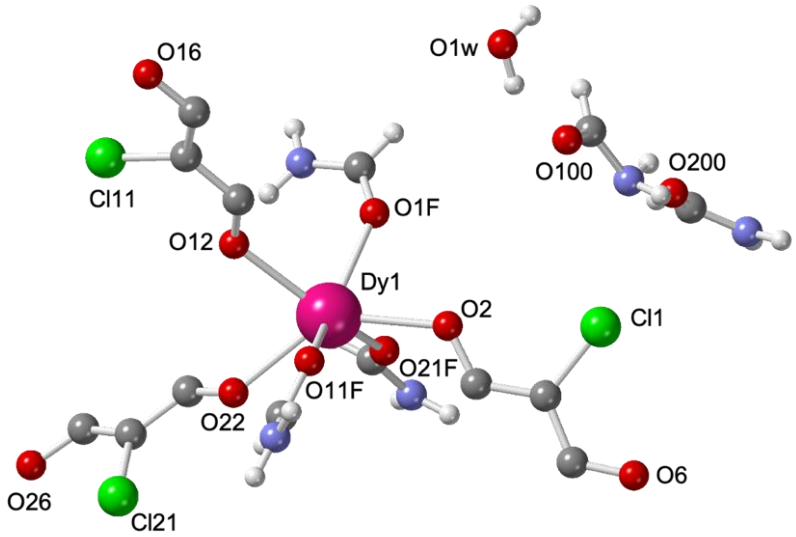

Figure S2. Asymmetric unit of compound $[Dy_2(C_6O_4Cl_2)_3(fma)_6]\cdot 4fma\cdot 2H_2O$ (**3**) showing the labelling scheme.

Table S1. Crystal data for compounds $[Dy_2(C_6O_4Cl_2)_3(fma)_6]\cdot 4.5fma$ (**1**), $[Dy_2(C_6O_4Br_2)_3(fma)_6]\cdot 4fma\cdot 2H_2O$ (**2**) and $[Dy_2(C_6O_4Cl_2)_3(fma)_6]\cdot 4fma\cdot 2H_2O$ (**3**).

Compound	**1**	**2**	**3**
CCDC	2329423	2329424	2329425
Empirical formula	$C_{12}H_4Cl_3DyN_3O_9$	$C_{14}H_{17}Br_3DyN_5O_{12}$	$C_{14}H_{17}Cl_3DyN_5O_{12}$
Formula weight	603.03	849.55	716.17
Temperature (K)	120.4(8)	120.00(10)	119.99(10)
Crystal system	monoclinic	monoclinic	monoclinic
Space group	$P2_1/c$	$P2_1/c$	$P2_1/c$
a (Å)	15.3308(9)	15.1035(6)	15.2098(7)
b (Å)	12.7233(5)	12.9448(3)	12.5682(4)
c (Å)	13.9678(10)	13.7837(4)	13.6608(6)
α (°)	90	90	90
β (°)	116.700(9)	114.866(4)	114.708(5)
γ (°)	90	90	90
Volume (Å^3)	2434.0(3)	2445.04(15)	2372.32(19)
Z	4	4	4
ρ_{calc} (g/cm^3)	1.646	2.308	2.005
μ (mm^{-1})	3.439	8.026	20.65
F(000)	1144.0	1612.0	1396.0
Crystal size (mm^3)	0.18×0.1×0.07	0.11×0.05×0.02	0.11×0.05×0.02
Radiation Mo Ka (l)	0.71073	0.71073	0.71073
2Θ range for data collection (°)	5.834-56.01	5.916-50.062	5.916-50.062
Index ranges	-19 ≤ h ≤ 15 -13 ≤ k ≤ 15 -18 ≤ l ≤ 14	-16 ≤ h ≤ 17 -14 ≤ k ≤ 15 -16 ≤ l ≤ 9	-18 ≤ h ≤ 17 -14 ≤ k ≤ 13 -16 ≤ l ≤ 16
Reflections collected	10051	8988	13582
Independent reflections	4955	4313	4174
R_{int}	0.0304	0.0376	0.0381
Independent reflections	0.0537	0.0594	0.0339
Data/restraints/parameters	4955/64/262	4313/208/305	4174/23/320
Goodness-of-fit on F^2	1.028	1.045	1.032
Final R indexes [I ≥ 2σ (I)]	R_1 = 0.0407	R_1 = 0.0390	R_1 = 0.0511
Final R indexes [all data]	wR_2 = 0.1103	wR_2 = 0.0897	wR_2 = 0.1367
Largest diff. peak/hole (e Å^{-3})	1.92/-1.48	1.24/-0.99	1.83/-1.17

Table S2. Bond distances for compounds $[Dy_2(C_6O_4Cl_2)_3(fma)_6]\cdot 4.5fma$ (**1**), $[Dy_2(C_6O_4Br_2)_3(fma)_6]\cdot 4fma\cdot 2H_2O$ (**2**) and $[Dy_2(C_6O_4Cl_2)_3(fma)_6]\cdot 4fma\cdot 2H_2O$ (**3**).

1		**2**		**3**	
Atoms	**distance (Å)**	**Atoms**	**distance (Å)**	**Atoms**	**distance (Å)**
Dy1-O2	2.392(4)	Dy1-O2	2.383(5)	Dy1-O12	2.391(4)
Dy1-O6^2	2.453(4)	Dy1-O6^4	2.432(5)	Dy1-O16^3	2.457(4)
Dy1-O12	2.385(4)	Dy1-O12	2.355(5)	Dy1-O26^6	2.419(4)
Dy1-O16^3	2.392(4)	Dy1-O16^5	2.396(5)	Dy1-O22	2.380(4)
Dy1-O22	2.380(4)	Dy1-O22	2.387(5)	Dy1-O2	2.363(4)
Dy1-O26^1	2.462(4)	Dy1-O26^3	2.449(4)	Dy1-O1F	2.351(5)
<Dy-O$_{anilato}$>	**2.411**	**<Dy-O$_{anilato}$>**	**2.400**	**<Dy-O$_{anilato}$>**	**2.394**
Dy1-O1F	2.350(4)	Dy1-O1F	2.470(5)	Dy1-O6^1	2.405(5)
Dy1-O11F	2.395(4)	Dy1-O11F	2.365(5)	Dy1-O21F	2.406(5)
Dy1-O21F	2.416(7)	Dy1-O21F	2.399(5)	Dy1-O11F	2.455(5)
<Dy-O$_{fma}$>	**2.387**	**<Dy-O$_{fma}$>**	**2.411**	**<Dy-O$_{fma}$>**	**2.422**

Symmetry operations: 1 = -x,1-y,-z; 2 = -x,1-y,1-z; 3 = 1-x,1-y,1-z; 4 = 1-x,1-y,2-z; 5 = 2-x,1-y,2-z and 6 = 1-x,1-y,-z.

Table S3. Bond angles for compounds $[Dy_2(C_6O_4Cl_2)_3(fma)_6]\cdot 4.5fma$(**1**), $[Dy_2(C_6O_4Br_2)_3(fma)_6]\cdot 4fma\cdot 2H_2O$ (**2**) and $[Dy_2(C_6O_4Cl_2)_3(fma)_6]\cdot 4fma\cdot 2H_2O$ (**3**).

1		**2**		**3**	
Atoms	**Angle(º)**	**Atoms**	**Angle(º)**	**Atoms**	**Angle(º)**
O2-Dy1-O26^1	69.17(13)	O6^4-Dy1-O26^3	127.28(15)	O12-Dy1-O16^3	65.39(14)
O2-Dy1-O6^2	65.15(13)	O6^4-Dy1-O1F	131.17(18)	O12-Dy1-O26^6	69.97(15)
O2-Dy1-O16^3	140.87(13)	O22-Dy1-O6^4	70.04(15)	O12-Dy1-O6^1	140.53(17)
O2-Dy1-O11F	137.42(14)	O22-Dy1-O26^3	65.37(15)	O12-Dy1-O21F	137.72(16)
O2-Dy1-O21F	76.4(2)	O22-Dy1-O16^5	139.30(16)	O12-Dy1-O11F	80.63(19)
O12-Dy1-O2	135.43(13)	O22-Dy1-O21F	137.69(17)	O26^6-Dy1-O16^3	127.19(15)
O12-Dy1-O26^1	139.17(14)	O22-Dy1-O1F	79.96(18)	O26^6-Dy1-O11F	131.65(19)
O12-Dy1-O6^2	71.00(13)	O26^3-Dy1-O1F	65.97(17)	O22-Dy1-O12	77.03(15)
O12-Dy1-O16^3	66.20(13)	O16^5-Dy1-O6^4	110.77(16)	O22-Dy1-O16^3	126.39(15)
O12-Dy1-O11F	75.86(14)	O16^5-Dy1-O26^3	121.19(16)	O22-Dy1-O26^6	65.35(14)
O12-Dy1-O21F	93.7(2)	O16^5-Dy1-O21F	69.08(18)	O22-Dy1-O6^1	68.98(15)
O22-Dy1-O2	81.46(14)	O16^5-Dy1-O1F	69.75(18)	O22-Dy1-O21F	98.18(17)
O22-Dy1-O12	136.89(14)	O11F-Dy1-O6^4	79.53(16)	O22-Dy1-O11F	71.30(17)
O22-Dy1-O26^1	64.42(13)	O11F-Dy1-O22	84.96(16)	O2-Dy1-O12	137.27(14)
O22-Dy1-O6^2	130.84(14)	O11F-Dy1-O26^3	70.13(16)	O2-Dy1-O16^3	71.97(15)
O22-Dy1-O16^3	70.70(14)	O11F-Dy1-O16^5	135.74(17)	O2-Dy1-O26^6	141.76(16)
O22-Dy1-O11F	89.44(16)	O11F-Dy1-O2	143.69(16)	O2-Dy1-O22	134.93(15)
O22-Dy1-O21F	71.3(2)	O11F-Dy1-O21F	75.55(18)	O2-Dy1-O6^1	67.01(15)
O1F-Dy1-O2	83.71(15)	O11F-Dy1-O1F	135.98(18)	O2-Dy1-O21F	74.45(16)
O1F-Dy1-O12	75.41(14)	O12-Dy1-O6^4	141.55(16)	O2-Dy1-O11F	85.08(19)
O1F-Dy1-O22	141.30(14)	O12-Dy1-O22	137.85(15)	O1F-Dy1-O12	84.64(16)
O1F-Dy1-O26^1	76.91(14)	O12-Dy1-O26^3	72.57(15)	O1F-Dy1-O16^3	69.97(16)
O1F-Dy1-O6^2	71.85(16)	O12-Dy1-O16^5	67.34(16)	O1F-Dy1-O26^6	79.34(15)
O1F-Dy1-O16^3	134.85(15)	O12-Dy1-O11F	78.38(16)	O1F-Dy1-O22	143.97(15)
O1F-Dy1-O11F	77.87(17)	O12-Dy1-O2	135.20(15)	O1F-Dy1-O2	78.27(16)
O1F-Dy1-O21F	138.3(2)	O12-Dy1-O21F	74.52(17)	O1F-Dy1-O6^1	134.83(17)
O6^2-Dy1-O26^1	126.44(13)	O12-Dy1-O1F	85.68(18)	O1F-Dy1-O21F	75.10(18)
O16^3-Dy1-O26^1	118.67(14)	O2-Dy1-O6^4	65.02(15)	O1F-Dy1-O11F	136.02(17)
O16^3-Dy1-O6^2	114.27(14)	O2-Dy1-O22	76.14(16)	O6^1-Dy1-O16^3	121.27(16)
O16^3-Dy1-O11F	70.65(15)	O2-Dy1-O26^3	125.75(16)	O6^1-Dy1-O26^6	110.97(15)
O16^3-Dy1-O21F	69.1(2)	O2-Dy1-O16^5	68.80(16)	O6^1-Dy1-O21F	68.56(19)
O11F-Dy1-O26^1	69.40(13)	O2-Dy1-O21F	98.04(17)	O6^1-Dy1-O11F	70.09(19)
O11F-Dy1-O6^2	139.51(15)	O2-Dy1-O1F	71.03(18)	O21F-Dy1-O16^3	135.35(16)
O11F-Dy1-O21F	139.2(2)	O21F- Dy1- O6^4	69.69(16)	O21F-Dy1-O26^6	70.04(16)
O21F-Dy1-O26^1	126.6(2)	O21F- Dy1- O26^3	136.16(17)	O21F-Dy1-O11F	138.33(19)
O21F-Dy1-O6^2	66.6(2)	O21F- Dy1- O1F	138.57(19)	O11F Dy1-O16^3	66.19(16)

Symmetry operations: 1 = -x,1-y,-z; 2 = -x,1-y,1-z; 3 = 1-x,1-y,1-z; 4 = 1-x,1-y,2-z; 5 = 2-x,1-y,2-z and 6 = 1-x,1-y,-z.

Table S4. Continuous SHAPE measurement (CShM) values of the 13 possible coordination geometries for the Dy^{III} ion with coordination number nine in compounds $[Dy_2(C_6O_4Cl_2)_3(fma)_6]\cdot 4.5fma$ (**1**), $[Dy_2(C_6O_4Br_2)_3(fma)_6]\cdot 4fma\cdot 2H_2O$ (**2**) and $[Dy_2(C_6O_4Cl_2)_3(fma)_6]\cdot 4fma\cdot 2H_2O$ (**3**).

Geometry	Symmetry	1	2	3
EP-9	D9h	36.753	37.136	36.982
OPY-9	C8v	22.294	22.760	22.795
HBPY-9	D7h	19.155	19.675	19.606
JTC-9	C3v	15.494	15.438	15.355
JCCU-9	C4v	10.087	9.579	9.389
CCU-9	C4v	8.891	8.350	8.200
JCSAPR-9	C4v	1.664	1.404	1.353
CSAPR-9	**C4v**	**0.649**	**0.388**	**0.378**
JTCTPR-9	D3h	2.072	2.330	2.298
TCTPR-9	D3h	0.671	0.767	0.796
JTDIC-9	C3v	12.545	12.067	12.218
HH-9	C2v	11.511	12.101	11.969
MFF-9	Cs	0.726	0.750	0.764

EP-9 = Enneagon; OPY-9 = Octagonal pyramid; HBPY-9 = Heptagonal bipyramid; JTC-9 = Triangular cupola (J3) = trivacant cuboctahedron; JCCU-9 = Capped cube (Elongated square pyramid, J8); CCU-9 = Capped cube; JCSAPR-9 = Capped square antiprism (Gyroelongated square pyramid J10); **CSAPR-9 = Capped square antiprism**; JTCTPR-9 = Tricapped trigonal prism (J51); TCTPR-9 = Tricapped trigonal prism; JTDIC-9 = Tridiminished icosahedron (J63); HH-9 = Hula-hoop; MFF-9 = Muffin. The lower value is highlighted in bold.

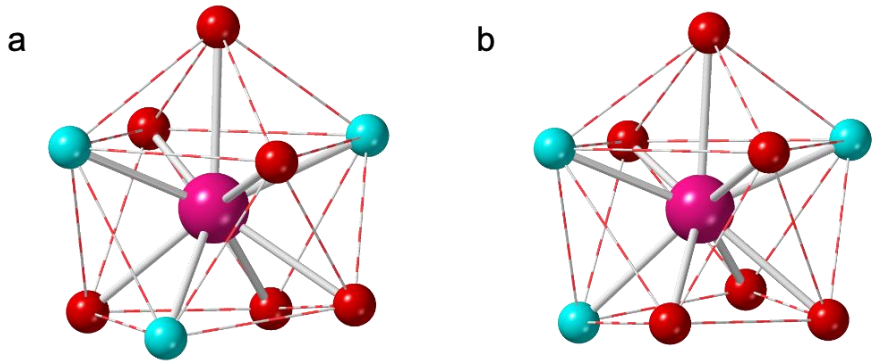

Figure S3. Coordination geometry in compounds: (**a**) $[Dy_2(C_6O_4Cl_2)_3(fma)_6]\cdot 4fma\cdot 2H_2O$ (**2**) and (**b**) $[Dy_2(C_6O_4Cl_2)_3(fma)_6]\cdot 4fma\cdot 2H_2O$ (**3**). Colour code: Dy = pink, $O_{anilato}$ = red, O_{fma} = light blue.

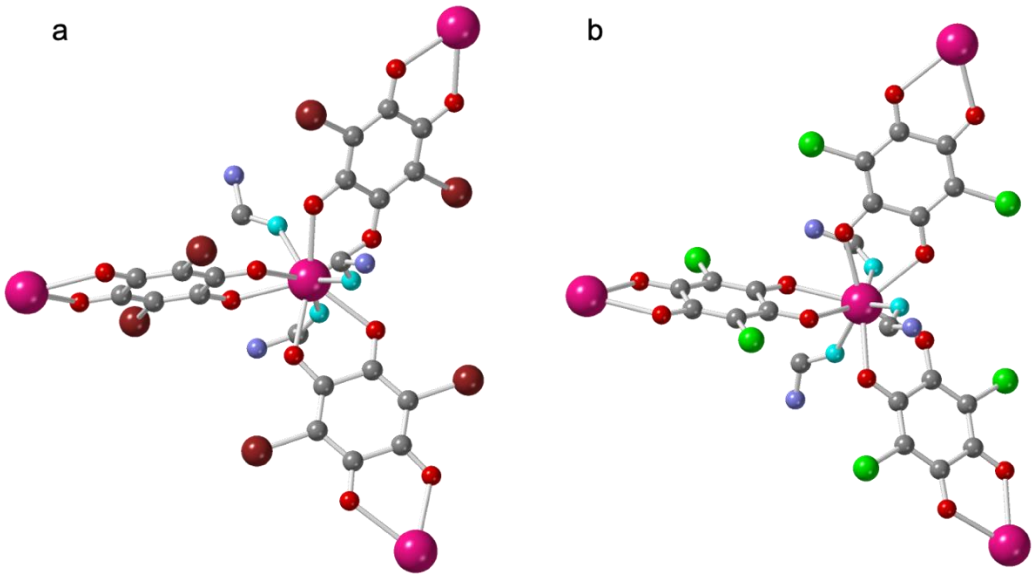

Figure S4. View of the coordination environment of the Dy centre in compounds: (**a**) $[Dy_2(C_6O_4Br_2)_3(fma)_6]\cdot 4fma\cdot 2H_2O$ (**2**) and (**b**) $[Dy_2(C_6O_4Cl_2)_3(fma)_6]\cdot 4fma\cdot 2H_2O$ (**3**). Colour code: Dy = pink, $O_{anilato}$ = red, O_{fma} = light blue, C = grey, Cl = green, Br = brown and N = dark blue. H atoms are omitted for clarity.

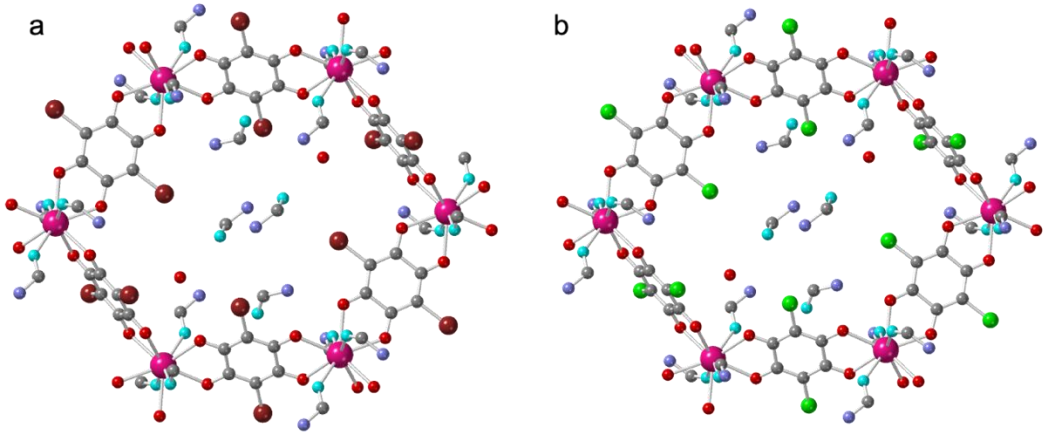

Figure S5. View of one hexagonal cavity in: (**a**) $[Dy_2(C_6O_4Br_2)_3(fma)_6]\cdot 4fma\cdot 2H_2O$ (**2**) and (**b**) $[Dy_2(C_6O_4Cl_2)_3(fma)_6]\cdot 4fma\cdot 2H_2O$ (**3**). Colour code: Dy = pink, $O_{anilato}$ = red, O_{fma} = light blue, C = grey, Cl = green, Br = brown and N = dark blue. H atoms are omitted for clarity.

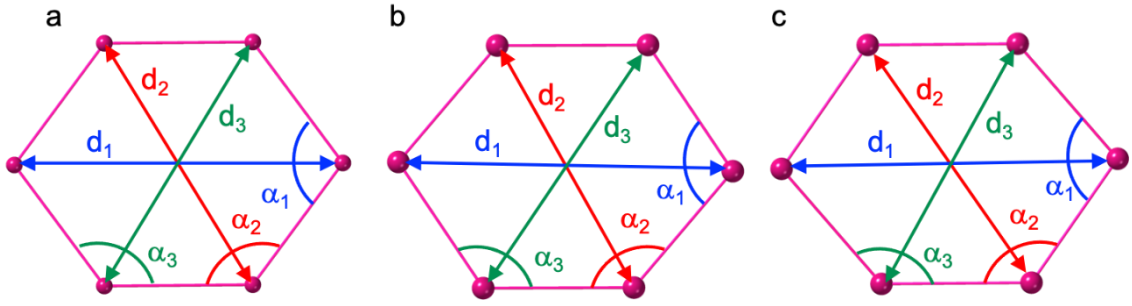

Figure S6. Schematic view of one hexagonal cavity in: (**a**) $[Dy_2(C_6O_4Cl_2)_3(fma)_6]\cdot 4.5fma$ (**1**), (**b**) $[Dy_2(C_6O_4Br_2)_3(fma)_6]\cdot 4fma\cdot 2H_2O$ (**2**) and (**c**) $[Dy_2(C_6O_4Cl_2)_3(fma)_6]\cdot 4fma\cdot 2H_2O$ (**3**). Dy^{III} atoms are represented by pink balls connected by pink lines that represent the anilato bridges. d_i are the diagonals of the hexagon and α_i are the Dy-Dy-Dy angles (values in Table S5).

Table S5. Dy-Dy distances (d_i), Dy-Dy-Dy angles (α_I, Figure S6) and the corresponding distortions in the hexagonal cavities in compounds $[Dy_2(C_6O_4Cl_2)_3(fma)_6]\cdot 4fma\cdot 8H_2O$ (**1**), $[Dy_2(C_6O_4Br_2)_3(fma)_6]\cdot 4fma\cdot 2H_2O$ (**2**) and $[Dy_2(C_6O_4Cl_2)_3(fma)_6]\cdot 4fma\cdot 2H_2O$ (**3**).

	1	**2**	**3**
d_1 (Å)	18.87	18.97	19.17
d_2 (Å)	16.51	16.71	16.54
d_3 (Å)	16.39	15.83	15.79
α_1 (º)	105.48	103.67	102.50
α_2 (º)	122.99	120.44	121.96
α_3 (º)	123.77	126.81	127.37
$\sum\lvert d_i - \bar{d}\rvert$ (Å)[a]	3.23	3.61	4.00
$\Sigma\ \lvert 120 - a_i\rvert$ (º)[b]	21.28	23.59	26.84

a = sum of the deviations from the average d value;
b = sum of the deviations from 120º.

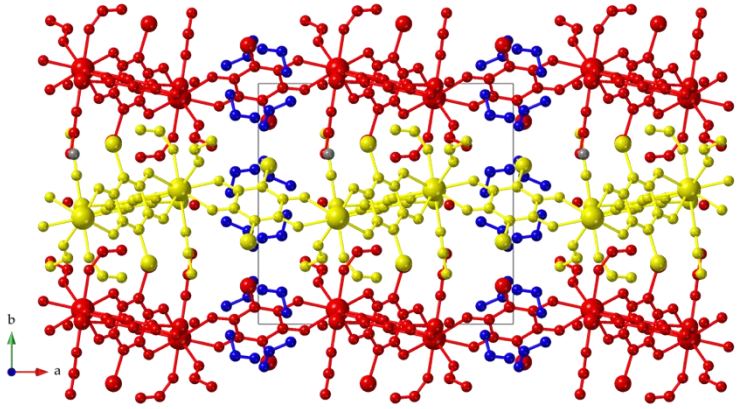

Figure S7. Side view, along the *b* axis, of three consecutive layers in compound $[Dy_2(C_6O_4Br_2)_3(fma)_6]\cdot 4fma\cdot 2H_2O$ (**2**) (represented in red, yellow and red). The crystallization fma molecules are shown in dark blue. H atoms are omitted for clarity

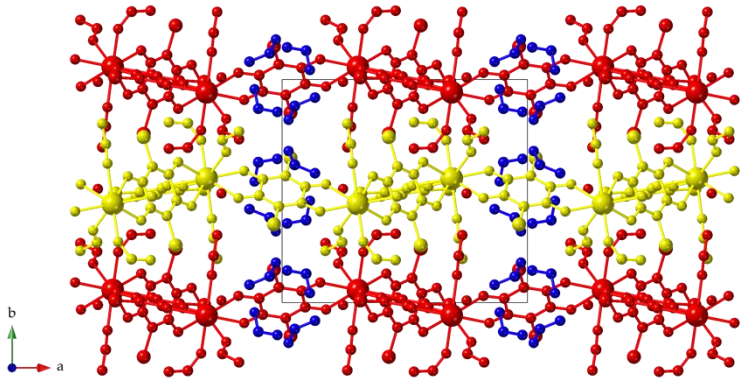

Figure S8. Side view, along the *b* axis, of three consecutive layers in compound $[Dy_2(C_6O_4Cl_2)_3(fma)_6]\cdot 4fma\cdot 2H_2O$ (**3**) (represented in red, yellow and red). The crystallization fma molecules are shown in dark blue. H atoms are omitted for clarity

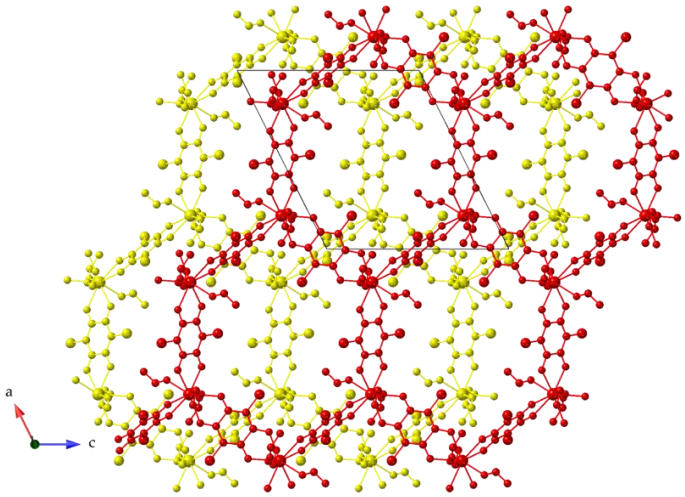

Figure S9. Projection of three consecutive layers in the *b* direction perpendicular to the layers in $[Dy_2(C_6O_4Cl_2)_3(fma)_6]\cdot 4.5fma$ (**1**). H atoms and crystallization solvent molecules are omitted for clarity.

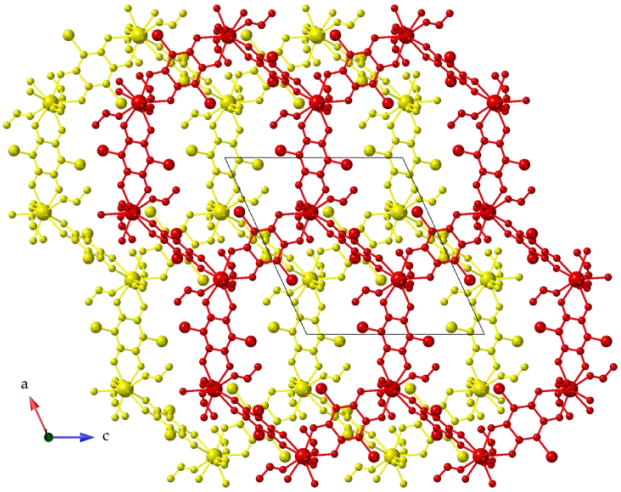

Figure S10. Projection of three consecutive layers in the direction perpendicular to the layers in $[Dy_2(C_6O_4Br_2)_3(fma)_6]\cdot 4fma\cdot 2H_2O$ (**2**). H atoms and crystallization solvent molecules are omitted for clarity.

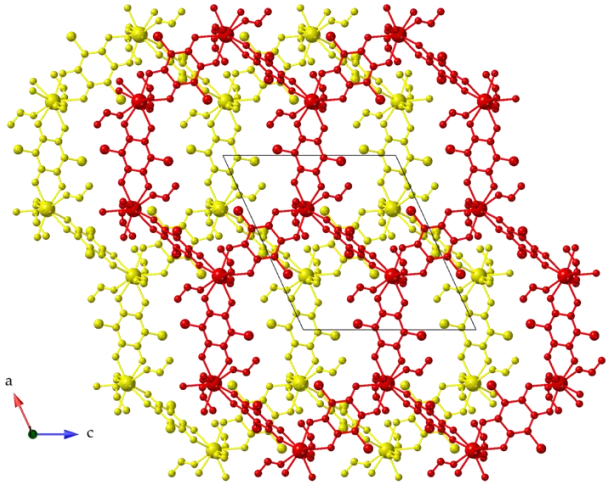

Figure S11. Projection of three consecutive layers in the direction perpendicular to the layers in $[Dy_2(C_6O_4Cl_2)_3(fma)_6]\cdot 4fma\cdot 2H_2O$ (**3**). H atoms and crystallization solvent molecules are omitted for clarity.

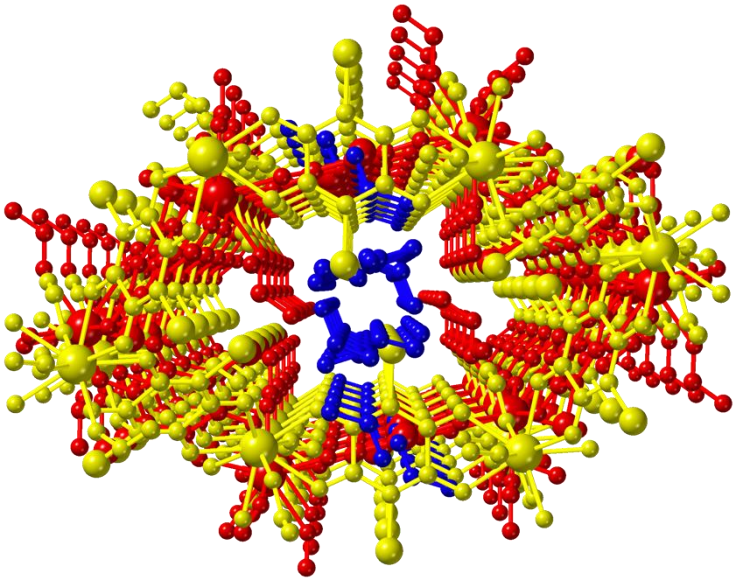

Figure S12. Perspective view of one channel formed along the [011] direction in $[Dy_2(C_6O_4Br_2)_3(fma)_6]\cdot 4fma\cdot 2H_2O$ (**2**). The crystallization fma molecules are shown in dark blue. H atoms are omitted for clarity.

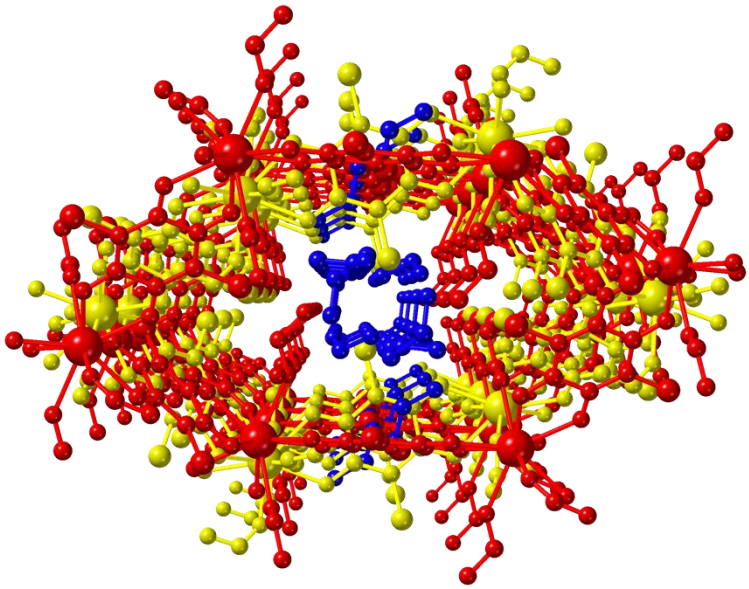

Figure S13. Perspective view of one channel formed along the [011] direction in $[Dy_2(C_6O_4Cl_2)_3(fma)_6]\cdot 4fma\cdot 2H_2O$ (**3**). The crystallization fma molecules are shown in dark blue. H atoms are omitted for clarity.

Table S6. H-contacts parameters in compound $[Dy_2(C_6O_4Br_2)_3(fma)_6]\cdot 4fma\cdot 2H_2O$ (**2**).

Atom1	Atom2	Symm. op. 1	Symm. op. 2	Length (Å)
N11F	O6	x,y,z	1-x,1-y,2-z	2.846
O6	O21F	x,y,z	1-x,1-y,2-z	2.761
O6	C21F	x,y,z	1-x,1-y,2-z	2.973
O16	O21F	x,y,z	2-x,1-y,2-z	2.720
O16	O1F	x,y,z	2-x,1-y,2-z	2.784
O2	O1F	1-x,1-y,2-z	1-x,1-y,2-z	2.821
O12	O11F	2-x,1-y,2-z	2-x,1-y,2-z	2.983
O12	O21F	2-x,1-y,2-z	2-x,1-y,2-z	2.878
O22	N11F	x,y,z	1-x,-1/2+y,1.5-z	3.049
Br11	O200	x,y,z	x,y,z	2.983
O1W	O100	x,y,z	x,y,z	2.841
O100	N100	x,y,z	2-x,1-y,1-z	3.019
N100	O200	x,y,z	x,y,z	2.980

Table S7. H-contacts parameters in compound $[Dy_2(C_6O_4Cl_2)_3(fma)_6]\cdot 4fma\cdot 2H_2O$ (**3**).

Atom1	Atom2	Symm. op. 1	Symm. op. 2	Length (Å)
N1F	O26	x,y,z	1-x,1-y,-z	2.834
O16	O1F	x,y,z	1-x,1-y,1-z	2.759
O16	O11F	x,y,z	1-x,1-y,1-z	2.681
O26	O21F	x,y,z	1-x,1-y,-z	2.770
O26	C21F	x,y,z	1-x,1-y,-z	2.959
C16	O11F	x,y,z	1-x,1-y,1-z	3.216
O22	O11F	1-x,1-y,-z	1-x,1-y,-z	2.819
O22	C11F	1-x,1-y,-z	1-x,1-y,-z	2.883
N1F	O12	x,y,z	1-x,-1/2+y,1/2-z	2.987
Cl1	O200	x,y,z	x,y,z	2.953
N11F	O1W	-x,1-y,-z	-x,-1/2+y,1/2-z	3.000
O200	N100	x,y,z	x,y,z	2.933
O1W	O100	x,y,z	x,y,z	2.819
O100	N100	x,y,z	-x,1-y,1-z	3.020

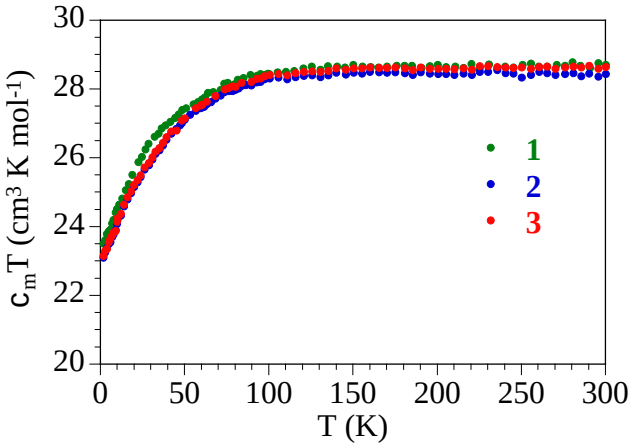

Figure S14. Thermal variation of the $\chi_m T$ product per formula unit for compounds $[Dy_2(C_6O_4Cl_2)_3(fma)_6]\cdot 4.5fma$ (**1**), $[Dy_2(C_6O_4Br_2)_3(fma)_6]\cdot 4fma\cdot 2H_2O$ (**2**) and $[Dy_2(C_6O_4Cl_2)_3(fma)_6]\cdot 4fma\cdot 2H_2O$ (**3**).

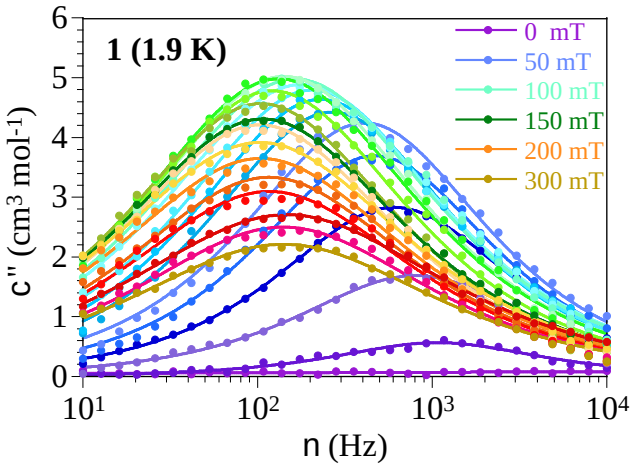

Figure S15. Frequency-dependence of the out of phase susceptibility (χ''_m) of compound $[Dy_2(C_6O_4Cl_2)_3(fma)_6]\cdot 4.5fma$ (**1**) at 1.9 K with different applied DC fields.

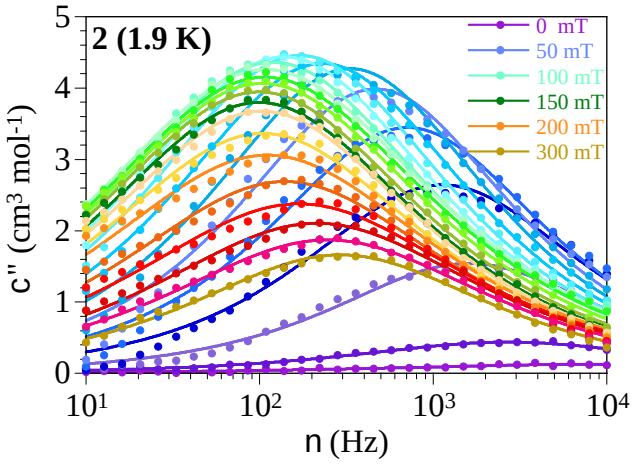

Figure S16. Frequency-dependence of the out of phase susceptibility (χ''_m) of compound $[Dy_2(C_6O_4Br_2)_3(fma)_6]\cdot 4fma\cdot 2H_2O$ (**2**) at 1.9 K with different applied DC fields.

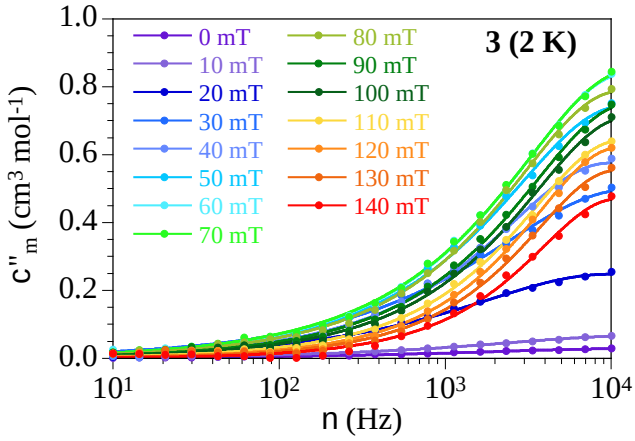

Figure S17. Frequency-dependence of the out of phase susceptibility (χ''_m) of compound $[Dy_2(C_6O_4Cl_2)_3(fma)_6]\cdot 4fma\cdot 2H_2O$ (**3**) at 2 K with different applied DC fields.

The field dependence of the relaxation time can be fitted to equation (1) with n = 4 for Kramers ions as Dy(III) with the parameters shown in table S8:[1]

$$\tau^{-1} = AH^nT + \frac{B_1}{1+B_2H^2} + D \qquad (1)$$

Table S8. Magnetic parameters obtained with equation (1) with n = 4 (fixed value), for compounds **1**-**3**.

Compound	A (s^{-1} K^{-1} mT^{-4})	B_1 (s^{-1})	B_2 (mT^{-2})	D (s^{-1})
1	3.8(2)x10^{-8}	8.6(2)x10^{3}	1.2(4)x10^{-3}	3.2(5)x10^{2}
2	1.1(2)x10^{-7}	2.95(3)x10^{8}	5.70(7)x10^{-1}	2.7(2)x10^{2}
3	3.0(2)x10^{-5}	3.1(2)x10^{4}	1.6(3)x10^{-3}	6.6(1)x10^{4}

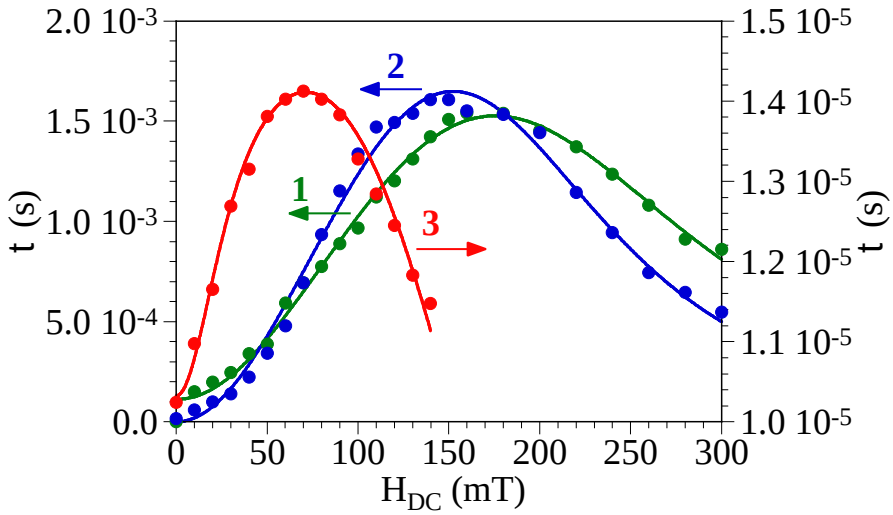

Figure S18. Dependence of the relaxation time (τ) with the DC field for compounds **1**-**3**. Solid lines are the best fit to the equation (1).

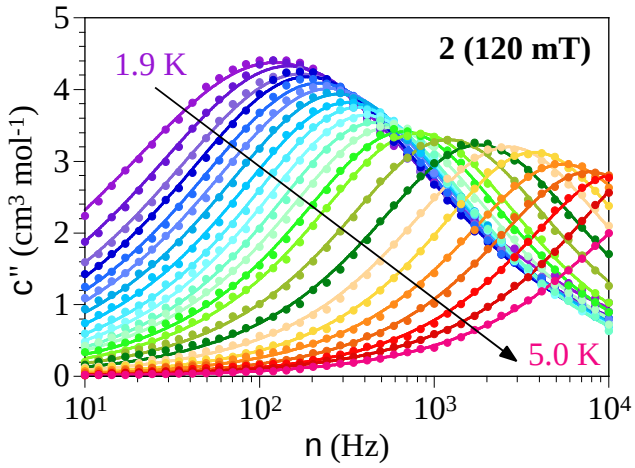

Figure S19. Frequency dependence of χ''_m for compound $[Dy_2(C_6O_4Br_2)_3(fma)_6]\cdot 4fma\cdot 2H_2O$ (**2**) at different temperatures with an applied DC field of 120 mT. Solid lines are the best fit to the Debye model.

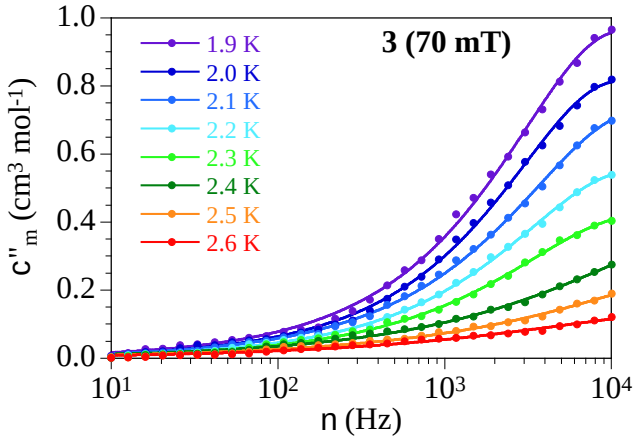

Figure S20. Frequency dependence of χ''_m for compound $[Dy_2(C_6O_4Cl_2)_3(fma)_6]\cdot 4fma\cdot 2H_2O$ (**3**) at different temperatures with an applied DC field of 70 mT. Solid lines are the best fit to the Debye model.

Table S9. Structural and magnetic parameters of all the reported Dy-anilate coordination polymers, including the three here reported.

CCDC	X	Solvent[b]	Structure[b]	c.n.	Geom.[c]	H_{dc} (mT)	U_{eff} (K)	Ref.
GEXGID	H	eg	3D-dia	9	TCTPR	60 100	49(1)/25(3) 36(1)/16(3)	2
GEXGOJ	Cl	eg	2D-brick	9	TCTPR	50 100	27(2)/19(4) 46(2)/32(1)	2
GEXGUP	Cl	eg/H_2O	3D-dia	9	TCTPR	60	37(1)	2
GEXHAW	Br	eg/MeOH	2D-hb	9	TCTPR	70	29.4(2)	2
GEXHEA	Br	eg	2D-brick	9	CSAPR	0 50	40.2(8) 39(1)/48(3)	2
GEXHIE	Br	eg	2D-brick	9	CSAPR	60	20(2)/47(3)	2
JUSBOR	Cl	MeOH	3D-dia	8	TDD	200	175(9)	3
JUSBIL	Cl	dmf	2D-hex	8	SAPR	200	145(7)	3
1565279	Br	H_2O	2D-hex	9	TCTPR	100	9.6(1)	4
LUTROK	Br	dmf	2D-hb	9	CSAPR	100	11.4(6)/(36(1)	4
NIDFUE	Br	dmso	2D-hex	8	TDD	100	22.8(4)	4, 5
NOQBON[d]	Br	dmso	2D-hb	9	CSAPR	0	40.9	6
UNOCUY	H	dmso/H_2O	2D-hex	8	TDD	60	17.1(9)	7
UNODAF	Cl	dmso	2D-hex	8	TDD	100	31.5(7)	7
XOYTUD	Cl/CN	dmso	2D-brick	9	CSAPR	100	21(3)	7, 8
1	Cl	fma	2D-hex	9	CSAPR	120	30(2)	This work
2	Br	fma/H_2O	2D-hex	9	CSAPR	120	41(1)	This work
3	Cl	fma/H_2O	2D-hex	9	CSAPR	70	42(7)	This work

(a) eg = ethylene glycol, dmf = dimethylformamide, dmso = dimethylsulfoxide; fma = formamide (b) dia = diamantine, brick = brick-wall (6,3), hb = herringbone (6,3), hex = hexagonal (6,3); (c) TCTPR = tri-capped trigonal prism, CSAPR = capped square antiprism, TDD = triangular dodecahedron, SAPR = square antiprism (d) 2 % Dy-doped Eu compound.

References

1. Dey, A.; Kalita, P.; Chandrasekhar, V. Lanthanide (III)-based single-ion magnets. *ACS omega* **2018***, 3*, 9462-9475.

2. Benmansour, S.; Pintado-Zaldo, C.; Martínez-Ponce, J.; Hernández-Paredes, A.; Valero-Martínez, A.; Gómez-Benmansour, M.; Gómez-García, C. J. The Versatility of Ethylene Glycol to Tune the Dimensionality and Magnetic Properties in DyIII-Anilato-Based Single-Ion Magnets. *Cryst. Growth Des.* **2023***, 23*, 1269-1280.

3. Mondal, A.; Roy, S.; Konar, S. Remarkable Energy Barrier for Magnetization Reversal in 3D and 2D Dysprosium-Chloranilate-Based Coordination Polymers. *Chem. Eur. J.* **2020***, 26*, 8774-8783.

4. Benmansour, S.; Hernandez-Paredes, A.; Mondal, A.; Lopez Martinez, G.; Canet-Ferrer, J.; Konar, S.; Gómez-García, C. J. Slow relaxation of the magnetization, reversible solvent exchange and luminescence in 2D anilato-based frameworks. *Chem. Commun.* **2020***, 56*, 9862-9865.

5. Benmansour, S.; Hernandez-Paredes, A.; Gómez-García, C. J. Effect of the lanthanoid-size on the structure of a series of lanthanoid-anilato 2-D lattices. *J. Coord. Chem.* **2018***, 71*, 845-863.

6. Hernandez-Paredes, A.; Cerezo-Navarrete, C.; Gómez García, C. J.; Benmansour, S. Slow relaxation in doped coordination polymers and dimers based on lanthanoids and anilato ligands. *Polyhedron* **2019***, 170*, 476-485.

7. Benmansour, S.; Hernandez-Paredes, A.; Bayona-Andres, M.; Gómez-García, C. J. Slow Relaxation of the Magnetization in Anilato-Based Dy(III) 2D Lattices. *Molecules* **2021***, 26*, 1190.

8. Sahadevan, S. A.; Monni, N.; Abherve, A.; Cosquer, G.; Oggianu, M.; Ennas, G.; Yamashita, M.; Avarvari, N.; Mercuri, M. L. Dysprosium Chlorocyanoanilate-Based 2D-Layered Coordination Polymers. *Inorg. Chem.* **2019***, 58*, 13988-13998.